Available online at www.sciencedirect.com
SCIENCE DIRECT®
Agricultural and Forest Meteorology 127 (2004) 131–141
AGRICULTURAL AND FOREST METEOROLOGY
www.elsevier.com/locate/agrformet

A model for scalar advection inside canopies and application to footprint investigation

Xuhui Lee*

School of Forestry and Environmental Studies, Yale University, 21 Sachem Street, New Haven, CT 06520, USA

Accepted 15 July 2004

Abstract

In this paper, a model is presented for scalar advection inside canopies. A key result is an advection/diffusion equation that captures the persistence effect of the diffusion plume from elevated sources through a near-field modifier. The model is applicable to various source configurations including line source, plane and canopy sources with finite fetch, and horizontally extensive canopy source. Model prediction agrees reasonably well with the observations of a line and a plane heat source in a wind tunnel canopy.

The two-dimensional flux footprint in the x–z plane in homogeneous turbulence is expressed in analytical form and that in canopy turbulence is computed from the numerical solution of the advection/diffusion equation. The footprint calculations suggest that inclusion of flow inhomogeneity leads to a stronger near-field effect than in homogeneous turbulence, resulting in a maximum contribution to the observed flux to come from sources further away from the measurement tower. The flux measured within the roughness sublayer is weighted more heavily by contributions from sources in the lower canopy in unstable conditions and from the upper canopy in stable conditions. The flux footprint is less sensitive to source height in neutral air than in stratified air. The cross-wind integrated footprint reported in the literature is a special case of the present model.

Keywords: Footprint; Canopy turbulence; Fetch; Advection

1. Introduction

The objective of this paper is to investigate the two-dimensional flux footprint function in the x–z plane for elevated sources inside a canopy, where x is the streamwise direction and z is height above the ground. Such a footprint function is useful for the interpretation of eddy flux measurement where the source density S (dimension $\mathrm{ML^{-3}T^{-1}}$, where M is the mass, L the length and T the time) varies both with x and z. As in all previous studies of flux footprint, the flow is assumed to be homogeneous in the x direction.

Mathematically, the vertical flux, F (dimension $\mathrm{ML^{-2}T^{-1}}$), of a scalar measured at position, (x_m, z_m),

* Tel.: +1 203 432 6271; fax: +1 203 432 5023.
E-mail address: xuhui.lee@yale.edu.

0168-1923/$ – see front matter © 2004 Elsevier B.V. All rights reserved.
doi:10.1016/j.agrformet.2004.07.009

is a weighted average of contributions from all upwind sources distributed in the $x-z$ plane,

$$F(x_m, z_m) = \int_{-\infty}^{x_m} \int_0^{\min(h, z_m)} S(x, z) g \times (x_m - x, z, z_m)\, \mathrm{d}z\, \mathrm{d}x \quad (1)$$

where h is canopy height, and g the footprint function (dimension L^{-1}). In the convolution calculation, the footprint is dependent upon horizontal separation distance between the measurement point and the source location, $x_m - x$, because of horizontal homogeneity of the flow, but is a function of both the measurement height z_m and the source height z because of vertical heterogeneity of the flow.

The footprint function must be positive, and is meaningful only if $z \leq h$,

$$g(x, z, z_m) > 0, \quad 0 < z \leq h, x > 0 \quad (2)$$

Here it is assumed that horizontal diffusion is negligible [models that include this yield a small contribution from the 'downwind' area (e.g. Kljun et al., 2002)]. Also g is a property of the flow and is independent of source configuration. This feature allows us to set up certain source configuration that is convenient for its numerical solution and for investigation of its general behavior. In the special case that S varies with z only, Eq. (1) becomes

$$F(x_m, z_m) = \left[\int_0^{\min(h, z_m)} S\, \mathrm{d}z\right] \times \left[\int_{-\infty}^{x_m} g(x_m - x, z, z_m)\, \mathrm{d}x\right] \quad (3)$$

Conservation of mass for a horizontally extensive canopy requires

$$F(x_m, z_m) = \int_0^{\min(h, z_m)} S\, \mathrm{d}z \quad (4)$$

A comparison of Eqs. (3) and (4) leads to another important property that the footprint function obeys

$$\int_0^{\infty} g(x, z, z_m)\, \mathrm{d}x = 1 \quad (5)$$

The first generation of footprint models is concerned with scalar diffusion from a ground-level plane source [(Leclerc and Thurtell, 1990; Schmid, 1994; Horst and Weil, 1992)]. Later studies have extended the investigation to canopy sources, relying on either random flight simulations [(Baldocchi, 1997; Rannik et al., 2002; Strong et al., 2004)] or numerical solutions of the deterministic advection/diffusion equation (Lee, 2003). Each approach has its unique advantages and weaknesses, and both are subject to the same kind of uncertainties inherent to the parameterization of canopy turbulence. The random flight technique uses fewer simplifying assumptions, while the deterministic approach can sometimes bring out certain physical processes (e.g., the role of the near-field effect, Fig. 1) more clearly.

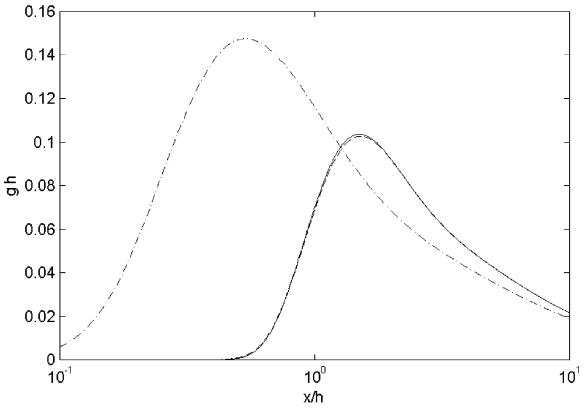

Fig. 1. Comparison of the numerical solution (dashed line) of the non-dimensional footprint function, $g(x, Z_1, z_m) \times h$, for homogeneous turbulence and the analytical solution (solid line, Eq. (27)), with $z_1/h = 0.8$, $z_m = 1.6$, $\tau u_*/h = 0.4$, $\sigma_w/u_* = 1.25$ and $u/u_* = 3$. Also given is a numerical solution with the near-field effect turned off (dash-dotted line).

In a companion paper, Lee (2003) combined Raupach et al. (1986) theory with parameterizations of the turbulence inside a canopy to investigate how air stability and source configuration influence the flux footprint and flux adjustment with fetch in the roughness sublayer. The footprint function investigated by Lee (2003) was essentially a source-weighted average of the two-dimensional version

$$g_s(x, z_m) = \frac{1}{\int_0^h S\, \mathrm{d}z} \int_0^h Sg\, \mathrm{d}z \quad (6)$$

Following Raupach (1989), the source term in the advection–diffusion equation was adjusted to account for the fact that the near-field concentration is advective but not diffusive. It must be recognized that the source-adjustment approach has not been verified

experimentally. While it appears adequate for the study of g_s, the approach is too crude for the study of the 2D footprint function, particularly its behavior in the near field.

In this study, a system of equations is established for scalar advection inside canopies. The point of departure is the problem of diffusion in homogeneous turbulence, which is reviewed in Section 2 to highlight mechanisms relevant to the process of advection/diffusion from elevated sources. Unlike Raupach (1989) whose theory targets primarily at horizontally homogeneous and extensive sources, the present study focuses on the advection/diffusion problem from line sources and plane sources with a finite fetch. The principal result is a conservation equation that incorporates the persistence of the diffusion plume in the near-field via a near-field modifier. The near-field modifier is assumed to take the same form in canopy turbulence, thus overcoming a closure problem (Section 3). The model is evaluated against observations of heat diffusion from a line source and a plane source in a wind tunnel canopy (Section 4). In Section 5, the basic equations for canopy turbulence are solved numerically to determinate the two-dimensional flux footprint, using a numerical procedure and canopy turbulence parameterization described by Lee (2003), for various stability conditions and measurement heights.

2. Scalar advection in homogeneous turbulence

2.1. Basic equations for a line source

2.1.1. Expressions for concentration and flux

Let us first consider an elemental line source, located at a height z_1 above the ground and horizontal position $x = 0$, in homogeneous turbulence specified by a horizontal velocity u, a standard deviation of the vertical velocity σ_w, and a Lagrangian time scale τ. The line source is infinitely long in the cross-wind direction. The line source function and the resulting concentration and flux fields are denoted by lowercase symbols, to distinguish from those for plane and canopy sources. The source function is

$$s = \delta_z(z_1)\delta_x(0) \tag{7}$$

where δ_z and δ_x are the Dirac delta functions. The analytical solution of concentration downwind of the source is given by

$$c(x,z;0,z_1) = \frac{1}{\sqrt{2\pi}\sigma_z u}\left\{\exp\left[-\frac{(z-z_1)^2}{2\sigma_z^2}\right] + \exp\left[-\frac{(z+z_1)^2}{2\sigma_z^2}\right]\right\} \tag{8}$$

(e.g., Csanady, 1973). The vertical flux, $f(x,z;0,z_1)$, is given by integrating the conservation equation, as

$$f(x,z;0,z_1) = -u\int_0^z \frac{\partial c}{\partial x}\,\mathrm{d}z \tag{9}$$

Substitution of Eq. (8) into Eq. (9) yields

$$f(x,z;0,z_1) = \frac{1}{\sqrt{2\pi}\sigma_z^2}\frac{\mathrm{d}\sigma_z}{\mathrm{d}x}\left\{(z-z_1)\exp\left[-\frac{(z-z_1)^2}{2\sigma_z^2}\right] + (z+z_1)\exp\left[-\frac{(z+z_1)^2}{2\sigma_z^2}\right]\right\} \tag{10}$$

where the plume depth σ_z is a function of x only and is obtained from

$$\sigma_z^2 = 2\sigma_w^2\tau\left\{\frac{x}{u} - \tau + \tau\exp\left(-\frac{x}{\tau u}\right)\right\} \tag{11}$$

and its derivative with respect to x is given by

$$\frac{\mathrm{d}\sigma_z}{\mathrm{d}x} = \frac{\sigma_w^2\tau}{\sigma_z u}\left\{1 - \exp\left(-\frac{x}{\tau u}\right)\right\} \tag{12}$$

Note that the solution of f does not invoke the gradient–diffusion relationship.

2.1.2. The far- and near-field concentrations

Following Raupach (1989), the concentration field c is separated into a diffusive far-field component c_f and a non-diffusive near-field component c_n

$$c = c_n + c_f \tag{13}$$

The far-field component satisfies the gradient–diffusion relationship

$$f = -K_f\frac{\partial c_f}{\partial z} \tag{14}$$

with the far-field diffusivity

$$K_f = \sigma_w^2\tau \tag{15}$$

Eq. (14) can be rearranged to give

$$c_f = \frac{1}{K_f}\int_z^\infty f\,dz \tag{16}$$

Substitution of Eq. (10) into Eq. (16) yields

$$c_f = \frac{d\sigma_z/dx}{\sqrt{2\pi}K_f}\left\{\exp\left[-\frac{(z-z_1)^2}{2\sigma_z^2}\right]+\exp\left[-\frac{(z+z_1)^2}{2\sigma_z^2}\right]\right\} \tag{17}$$

It can be shown from Eqs. (8) and (17) that the near-field component is related to the far-field component as

$$c_n \equiv c - c_f = \frac{\exp(-x/\tau_1 u_1)}{1-\exp(-x/\tau_1 u_1)}c_f \tag{18}$$

where $u_1 = u(z_1)$ and $\tau_1 = \tau(z_1)$. This equation has the desired property that as x increases the near-field concentration decreases rapidly. The reader should be aware that local values of wind speed and the Lagrangian time scale are used in Eq. (18). In the case of homogeneous turbulence discussed here, these values are constant with height. In the later treatment of inhomogeneous turbulence, this ensures that the boundary condition that the near-field effect, hence the near-field concentration, vanishes for a ground-level source, is satisfied.

2.2. Extension to a plane source

The above result can be easily extended to an elemental plane source. The source function in this case is given by

$$S = \begin{cases} \delta_z(z_1), & x > 0, \\ 0, & x \le 0 \end{cases} \tag{19}$$

The corresponding concentration fields (total concentration C, far-field concentration C_f and near-field concentration C_n) are obtained by the principle of superposition, as

$$\begin{aligned} C(x,z;z_1) &= \int_0^x c\,dx, \\ C_n(x,z;z_1) &= \int_0^x c_n\,dx, \\ C_f(x,z;z_1) &= \int_0^x c_f\,dx, \end{aligned} \tag{20}$$

It can be shown that substitution of Eqs. (17) and (18) into Eq. (20) gives C_n that is identical to that of Raupach (1989) in homogeneous turbulence in the limit $x \to \infty$. In canopy flow where the turbulence is vertically heterogeneous, the present treatment predicts a stronger near-field effect than Raupach (1989).

Eq. (20) is useful only if solutions for the elemental line source are known (as is the case for homogeneous turbulence). More generally, a solution for the plane source should be sought from the mass conservation equation

$$u\frac{\partial C}{\partial x} + \frac{\partial F}{\partial z} = S \tag{21}$$

and the gradient–diffusion relation

$$F(x,z;z_1) = -K_f\frac{\partial C_f}{\partial z} \tag{22}$$

where F is the vertical flux from the plane source. In Eq. (21), both the near- and far-field concentrations are advective, but only the far-field concentration is diffusive. A closure problem now exists because there are three unknowns (F, C and C_f) with only two equations. This problem is overcome by first taking the derivative of Eq. (20) with respect to x

$$c = \frac{\partial C}{\partial x}, \qquad c_n = \frac{\partial C_n}{\partial x}, \qquad c_f = \frac{\partial C_f}{\partial x} \tag{23}$$

Next Eqs. (17), (18), (20), (21) and (23), and

$$C = C_n + C_f \tag{24}$$

are manipulated to eliminate C. The final result is

$$\left[1+\frac{\exp(-x/\tau_1 u_1)}{1-\exp(-x/\tau_1 u_1)}\right]u\frac{\partial C_f}{\partial x} = \frac{\partial}{\partial z}\left(K_f\frac{\partial C_f}{\partial z}\right) + S \tag{25}$$

Eq. (25), which is exact in homogeneous turbulence, captures the near-field effect by including the group

$$\left[1+\frac{\exp(-x/\tau_1 u_1)}{1-\exp(-x/\tau_1 u_1)}\right]$$

called here as near-field modifier, in the advection term.

2.3. An analytical solution of flux footprint

An exact solution of the flux footprint function exists under the assumption of homogeneous turbulence, noting that substitution of Eq. (7) into Eq. (1) gives

$$f(x_m, z_m; 0, z_1) = g(x_m, z_1, z_m) \tag{26}$$

Thus the exact solution is

$$g(x, z_1, z_m) = \frac{1}{\sqrt{2\pi}\sigma_z^2}\frac{d\sigma_z}{dx}\left\{(z_m - z_1)\exp\left[-\frac{(z_m - z_1)^2}{2\sigma_z^2}\right] + (z_m + z_1)\exp\left[-\frac{(z_m + z_1)^2}{2\sigma_z^2}\right]\right\} \tag{27}$$

This function satisfies the conditions specified by Eqs. (2) and (5).

Eq. (27) is useful in two ways. First, it is used to check the accuracy of the numerical procedure described below (Section (3.3)). Second, an appreciation of the impact of flow inhomogeneity on the footprint function is gained by comparing the analytical solution with numerical calculations for inhomogeneous turbulence (Section (5.1)).

3. Scalar advection in canopy turbulence

3.1. Basic equations

Let us consider the same source configuration given by Eq. (19). In an idealized canopy flow, the turbulence is homogenous horizontally but not vertically. To overcome the closure problem, we assume that the near-field modifier has the same form of that pertaining to homogeneous turbulence so that Eq. (25) can be used to achieve a numerical solution of C_f. It is worth mentioning that while Eq. (25) is now an approximation, Eq. (20) and its derivative form, Eq. (23), are exact as long as the turbulence is horizontally homogeneous. Therefore, once the plane source solution is known, it can be manipulated to give the line source solution. This is a useful feature for model validation because line sources are used much more frequently than plane sources in diffusion experiments.

Once C_f is known, the vertical flux F is obtained from Eq. (22) with the far-field eddy diffusivity given by Eq. (15), and C_n and C are given by

$$C_n = \int_0^x \frac{\exp(-x/\tau_1 u_1)}{1 - \exp(-x/\tau_1 u_1)}\frac{\partial C_f}{\partial x}\,dx \tag{28}$$

and Eq. (24).

To determine the footprint function, we take advantage of the fact that for the source configuration specified by Eq. (19), Eq. (1) can be written as

$$F(x_m, z_m; z_1) = \int_0^{x_m} g(x_m - x, z_1, z_m)dx \tag{29}$$

Therefore, the footprint function is obtained by differentiating F with respect to x_m,

$$g(x_m, z_1, z_m) = \frac{\partial F(x_m, z_m; z_1)}{\partial x_m} \tag{30}$$

The present treatment differs from Raupach (1989), who overcomes the closure problem via a slight modification of the source term

$$u\frac{\partial C_f}{\partial x} = \frac{\partial}{\partial z}\left(K_f\frac{\partial C_f}{\partial z}\right) + S^* \tag{31}$$

where S^* is related to the real source strength S as

$$S^* = \begin{cases} 0 & \text{for } x \le u\tau, \\ S & \text{for } x > u\tau \end{cases} \tag{32}$$

The source-adjustment approach appears adequate for the source-weighted footprint function (Eq. (6)) but is too crude for the determination of the two-dimensional footprint, in part because of the discontinuity at $x = u\tau$. Eq. (25) does not suffer this shortcoming.

3.2. Parameterization of canopy turbulence

In the investigation of the effects of air stability and measurement height on the footprint function, the parameterizations in Lee (2003) are used for profiles of the horizontal velocity u, the standard deviation of the vertical velocity σ_w, and the Lagrangian time scale τ. Briefly, τ is parameterized according to Legg et al. (1986) for neutral air and Leuning (2000) for stratified air. All the parameters are made non-dimensional by canopy height, h, and friction velocity, u_*, and are functions of non-dimensional height z/h and a stability parameter ζ (= h/L, where L is the Monin–Obukhov length). In the model validation against wind tunnel observations (Section 4), the same parameterization of τ for neutral air is used together with the

observed profiles of u and σ_w reported by Raupach et al. (1986).

3.3. Numerical method

To establish the footprint function, we begin by specifying z_1 (source height), z_m (measurement height) and the stability parameter ζ. Eq. (25) is discretized according to Patankar (1980) and the solution for C_f is sought with a line-by-line method in the forward wind direction. The procedure is repeated for a number of preset z_1 values covering the range 0– h.

The boundary conditions are

$$C_f = 0, \quad x = 0; \qquad \frac{\partial C_f}{\partial z} = 0, \quad z = 0 \text{ and } 40h \tag{33}$$

The same numerical scheme is used in the model validation against the observation by Coppin (1986) of heat advection from a plane source in a wind tunnel canopy. For comparison with the observation by Legg et al. (1986) of heat advection from a line source in the same wind tunnel canopy, a solution is first sought for an elemental plane source placed at the same height as the line source ($z_1/h = 0.85$). Next a solution of the concentration fields for an elemental line source is obtained by differentiating the plane source solution with respect to x (Eq. (23)). After that, the vertical flux is obtained from Eq. (14). Finally, the elemental line source solution is scaled by the heat release rate and is compared with the actual observation.

Fig. 1 shows that the numerical solution of g for homogeneous turbulence is virtually identical to the analytical solution (Eq. (27)), indicating that the numerical procedure is sufficiently accurate for footprint investigation. Also shown in Fig. 1 is a solution with the near-field modifier set to unity, which is equivalent to turning off the near-field effect. Without the near-field effect, the footprint function displays a much higher peak at a position much closer to the observational point than the actual footprint function.

4. Comparison with experimental data

Figs. 2 and 3 compare the model predictions of temperature and vertical heat flux with actual observations downwind of a line source in a wind tunnel canopy (Legg et al., 1986). The temperature scale is defined as

$$\theta_* = \frac{Q_s}{\rho c_p h u_*}$$

where Q_s is the line source strength (in W m^{-1}), ρ and c_p are the air density and specific heat of air at constant pressure, respectively, and u_* the friction velocity. In the air layer in the upper canopy and higher, there is very good agreement between the calculated and observed temperature both in the near and far fields. The model underestimates temperature in the lower canopy in the near-field ($x/h = 0.38$ and 1.32). Legg et al. (1986) and Flesch and Wilson (1992) also reported similar underestimation by their random flight simulation models. It appears that either parameterization of the turbulence in the lower canopy is inaccurate in all these modeling studies or the measurement was in error.

Fig. 3 provides a direct experimental test of the footprint prediction, keeping in mind that the vertical flux field resulting from a line source is equivalent to the footprint function (Eq. (26)). Overall, the shape of

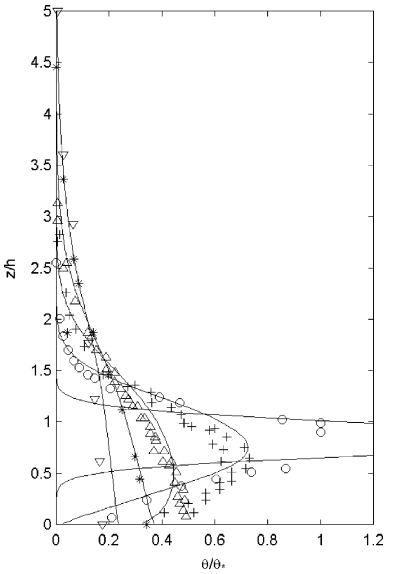

Fig. 2. Profiles of normalized temperature downwind of a heat line source in a wind tunnel canopy. Source height is $z/h = 0.85$. Symbols are observations at various distances from the source (circles, $x/h = 0.38$; crosses, 1.32; triangles, 2.78; asterisks, 5.72; upside down triangles, 11.6). Lines represent numerical solution at the same distances.

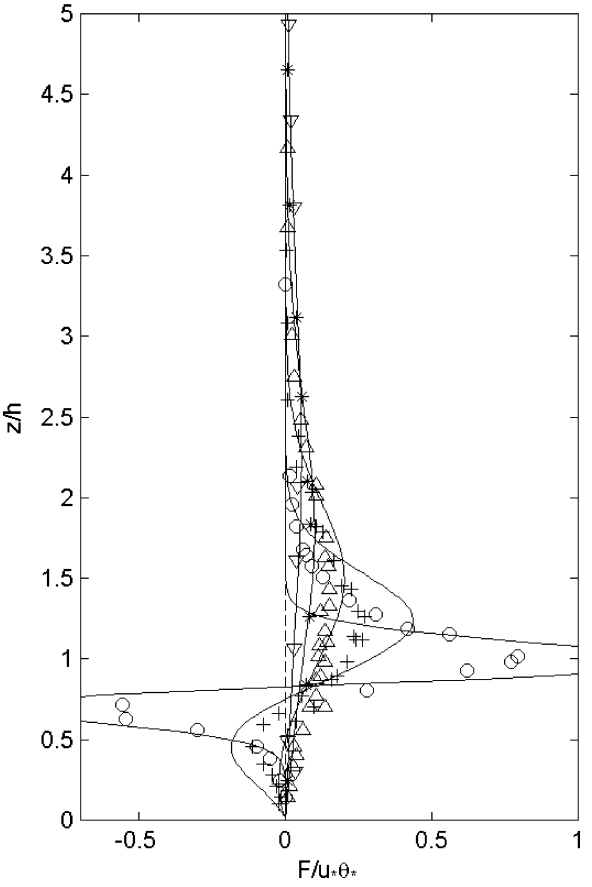

Fig. 3. As in Fig. 2 but for normalized vertical heat flux.

the predicted profile curves looks quite similar to the observed shape. The model prediction misses a few quantitative details, the most noticeable one being a large flux peak predicted by the model very close to the source ($x/h = 0.38$).

Fig. 4 compares the temperature and vertical flux profiles at a distance of $x/h = 33.8$ from the leading edge of a plane source in the same wind tunnel canopy (Coppin, 1986). This is the longest fetch distance at which the observation was made. Profiles at other shorter fetch distances are deemed less suitable for the comparison because the flow field was not fully adjusted with fetch. The temperature scale is defined as

$$\theta_* = \frac{H_s}{\rho c_p u_*}$$

where H_s is the plane source strength (in W m^{-2}). The agreement is excellent for the heat flux up to a height

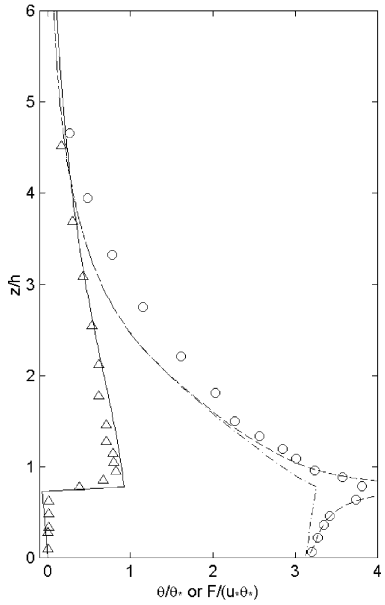

Fig. 4. Comparison of modeled profiles of temperature (dashed line) and vertical heat flux (solid line) with those observed in a wind tunnel canopy with a plane heat source (circles, temperature; triangles, heat flux). Dash-dotted line is the modeled far-field concentration profile. Source height is $z/h = 0.8$.

of $z/h = 4.5$ and for temperature up to a height of $z/h = 1.5$. Warland and Thurtell (2000) also reported similar disagreement with their model and suggested that it was caused by measurement errors. According to their calculations, Raupach (1989) theory appeared to underestimate the near-field effect in this canopy. In comparison, the near-field effect (the difference between the dashed and dash-dotted lines, Fig. 4) of this model is more pronounced, which improves the model prediction.

5. Results for flux footprint

5.1. Behavior of the 2D footprint function

Fig. 5 is a contour plot of the footprint function based on Eq. (27) for a measurement height of $z_m/h = 1.6$, with the u, τ and σ_w values taken at the source height from those specified for canopy turbulence in neutral air. The actual numerical solution for the canopy flow is presented in Fig. 6. The solution for homogeneous turbulence predicts that

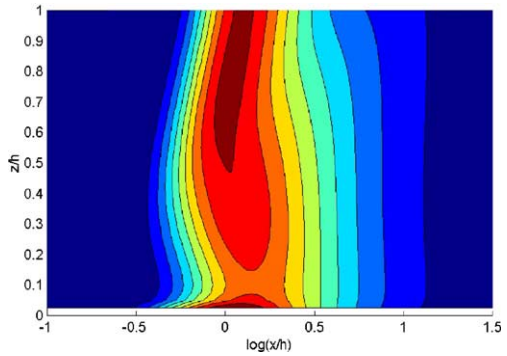

Fig. 5. Contour plot of the normalized footprint function, gh, from the analytical solution for homogeneous turbulence. Measurement height is $z_m/h = 1.6$. The maximum value of gh is 0.142. Contour interval is 0.014.

the maximum contribution to the observed flux comes from sources at a distance of $x/h = 1$ upwind whereas the numerical solution suggests the maximum at $x/h = 2$. The persistence of the diffusion plume (or the near-field effect) is stronger in the vertically inhomogeneous turbulence, causing the position of the maximum contribution to locate further upwind.

The effect of measurement height on the footprint function is illustrated in Fig. 7 for neutral air. At a measurement height close to the canopy top ($z_m/h = 1.2$), the flux is weighted more heavily by contributions from the sources in the upper canopy. In the upper roughness sublayer (Fig. 6) and inertial sublayer (Fig. 7, top panel), the flux footprint is not very sensitive to z. The vertical extent of the roughness sublayer is set at $z/h = 2.16$. At this height the

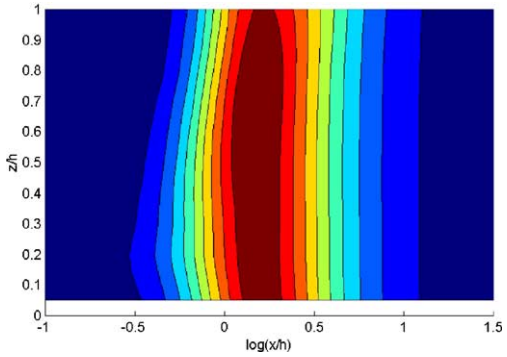

Fig. 6. As in Fig. 5 but from the numerical solution of canopy turbulence in neutral stability. The maximum value of gh is 0.159. Contour interval is 0.016.

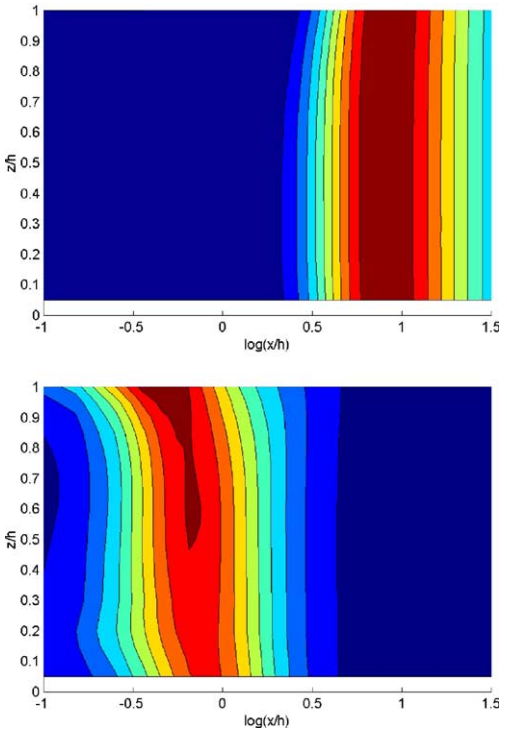

Fig. 7. Contour plot of the normalized footprint function, gh, in neutral stability. Bottom: measurement height $z_m/h = 1.2$, maximum 0.44, contour interval 0.044; top: measurement height $z_m/h = 3.0$, maximum 0.027, contour interval 0.0027.

Lagrangian time scale of the roughness sublayer matches its inertial sublayer form (Lee, 2003).

The insensitivity to z is, however, limited to near-neutral stability. In moderately unstable air ($\zeta = -1$, Fig. 8, bottom panel), the eddy time scale becomes relatively large, particularly in the upper canopy. The persistence of the diffusion plume emanating from the upper canopy is much stronger than that from the lower canopy. Consequently, the footprint contour shows an upwind tilt, The maximum contributions come from the lower canopy at $x/h = 0.3$.

In stable air, the tilt structure reverses direction and is much more pronounced than in unstable air ($\zeta = 1$, Fig. 8, top panel). The near-field effect is far outweighted by the fact that diffusion is very slow in stable air and thus it takes the diffusion plume a long time to influence the measurement if the vertical separation distance between z_m and the source height is large. These patterns are broadly consistent with the model calculations made by Baldocchi (1997).

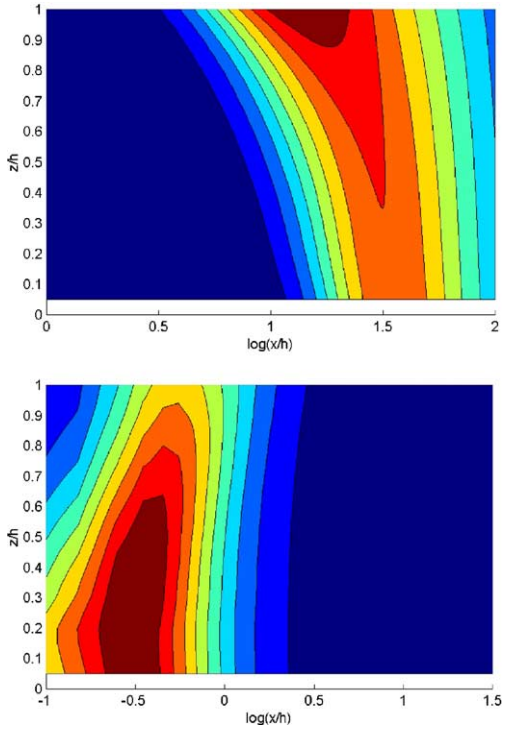

Fig. 8. Contour plot of the normalized footprint function, gh, for a measurement height $z_m/h = 1.6$. Bottom: unstable ($\zeta = -1$), maximum 0.85, contour interval 0.085; top: stable ($\zeta = 1$), maximum 0.0094, contour interval 0.00094.

5.2. Comparison with published models

The cross-wind integrated footprint function studied by Leclerc and Thurtell (1990) and Horst and Weil (1992) and others can be considered as a special case of the present model. These studies imply that the source distribution is a function of x only. If we express

$$S_0(x) = hS(x) \tag{34}$$

as the total surface source strength (dimension $\mathrm{ML^{-2}T^{-1}}$), we can rewrite Eq. (1) as

$$F(x_m, z_m) = \int_{-\infty}^{x_m} S_0(x) \left[\frac{1}{h} \int_0^h g(x_m - x, z, z_m) \mathrm{d}z \right] \mathrm{d}x \tag{35}$$

where $z_m > h$. Thus, the cross-wind integrated footprint function is essentially the algebraic average of

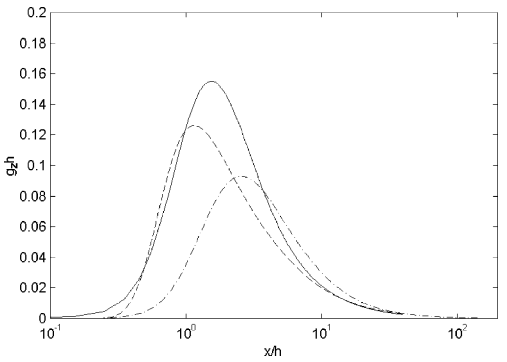

Fig. 9. Comparison of three estimates of the cross-wind integrated footprint function for a measurement height $z_m/h = 1.6$ and neutral stability: solid line, numerical solution; dashed line, analytical solution; dash-dotted line, solution based on the Monin–Obukhov similarity.

the two-dimensional function along the vertical direction, g_z (dimension L^{-1}),

$$g_z(x, z_m) = \frac{1}{h} \int_0^h g(x, z, z_m) \, \mathrm{d}z \tag{36}$$

Fig. 9 compares three estimates of the cross-wind integrated footprint function for a measurement height of $z_m/h = 1.6$ and neutral stability. In method 1, the numerical solution of g is integrated according to Eq. (36) (solid line). In method two, a solution is computed from the homogeneous turbulence solution (Eq. (27)), using values of u, σ_w and τ taken from those specified from canopy flow at various depths inside the canopy, and is integrated according to Eq. (36) (dashed line). In method three, the cross-wind integrated footprint function is solved numerically using the advection–diffusion equation for the atmospheric surface layer and the Monin–Obukhov similarity functions of the diffusivity and the wind profiles [Model II in Lee, 2003, dash-dotted line]. The first two methods account for the near-field effect. Even with the crude assumption of homogeneous turbulence, method two does a better job than method three. The poor performance of method three is caused by the lack of the near-field effect and its poor representation of the turbulence in the roughness sublayer. The solution based on the Monin–Obukhov similarity is clearly inadequate in the roughness sublayer.

6. Conclusions

In this paper, a model is presented for scalar advection inside canopies. The core equations are the mass conservation equation involving the far-field concentration (Eq. (25)), the flux–gradient relationship (Eq. (22)) and an expression for the near-field concentration (Eq. (28)). The persistence of the diffusion plume in the near-field is captured by a near-field modifier in the conservation equation. The near-field concentration is identical to that of Raupach (1989) in homogeneous turbulence and is stronger than the latter in vertically inhomogeneous turbulence. The model prediction of temperature and heat flux agrees reasonably well with the observations of a line and a plane heat source in a wind tunnel canopy.

Although the present study emphasizes an elemental plane source with a step change at the leading edge (Eq. (19)), by principle of superposition these equations should be applicable in the more general case of a canopy source whose source density S is an arbitrary function of both x and z, as long as the flow is horizontally homogeneous. The classic case of advection-free, horizontally extensive and homogeneous canopy, which is of interest to some modelers, is further discussed in Appendix A.

The numerical scheme developed for the plane source is a convenient intermediate step for canopy source as well as line source problems. The two-dimensional footprint function covering the full vertical extent of a canopy is constructed from the plane source solution by adjusting successively the plane source height. The solution for a line source is obtained by differentiating the solution for a plane source placed at the height of the line source (Eq. (23)). The ability to obtain a line source solution is a useful feature for model validation because line sources are used much more frequently in diffusion experiments than plane sources.

An analytical solution is derived for the footprint function in homogeneous turbulence. Flux footprint in canopy turbulence is computed from the numerical solution of the governing equations discussed above. According to the footprint calculations, the flux measured within the roughness sublayer is weighted more heavily by contributions from sources in the lower canopy in unstable conditions and from the upper canopy in stable conditions. The flux footprint is less sensitive to source height in neutral air.

The cross-wind integrated footprint reported in the literature is a special case of the present model. Model intercomparison (Fig. 9) and numerical experiments (Fig. 1) show that accounting for the persistence of the diffusion plume in the near-field is crucial for the determination of the flux footprint of elevated sources.

Acknowledgements

This work was supported by the U.S. National Science Foundation through grant ATM-0072864 and by the Biological and Environmental Research Program (BER), U.S. Department of Energy, through the northeast regional center of the National Institute for Global Environmental Change (NIGEC) under Cooperative Agreement No. DE-FC03-90ER61010.

Appendix A. The case of an advection-free, horizontally homogeneous canopy

The above theory can be extended to an extensive canopy whose source strength is a function of height only. In this case, horizontal advection vanishes. The far-field concentration reaches the equilibrium value given by

$$C_{\mathrm{f}}(z) - C_{\mathrm{f}}(z_{\mathrm{r}}) = \int_{z}^{z_{\mathrm{r}}} \frac{1}{K_{\mathrm{f}}(z')} \left[\int_{0}^{z'} S(z'')\, \mathrm{d}z'' \right] \mathrm{d}z' \tag{A.1}$$

(Raupach, 1989), where z_{r} is a reference height.

The solution for C_{n} is found numerically in a two-step process. First, a non-equilibrium C_{f} is solved from Eq. (25) with the boundary conditions specified by Eq. (33) and

$$S = \begin{cases} 0 & \text{for } x \le 0, \\ S(z) & \text{for } x > 0 \end{cases} \tag{A.2}$$

Next, the non-equilibrium C_{f} is put into Eq. (28) to give a solution for C_{n}. Theoretically, to reach the equilibrium solution for C_{n}, the integration limit in Eq. (28) should be infinitely large. But because the near-field modifier decays exponentially with x, it is found that an integration limit of $5h$ is sufficient.

The present theory appears to improve the prediction of the concentration profile in comparison to Raupach's original theory which is shown to underestimates the near-field effect (Warland and Thurtell, 2000). The improvement comes at the cost of a numerical approach that is somewhat cumbersome, although this is not a serious limitation given the computing power offered by today's desktop computers.

References

Baldocchi, D., 1997. Flux footprints within and over forest canopies. Bound.-Layer Meteorol. 85, 273–292.

Coppin, P.A., Raupach, M.R., Legg, B.J., 1986. Experiments on scalar dispersion within a model plant canopy. Part II. An elevated plane source. Bound.-Layer Meteorol. 35, 167–191.

Csanady, G.T., 1973. Turbulent Diffusion in the Environment. D. Reidel Publishing Company, Boston, MA, 248 pp.

Flesch, T.K., Wilson, J.D., 1992. A two-dimensional trajectory-simulation model for non-Gaussian, inhomogeneous turbulence within plant canopies. Bound.-Layer Meteorol. 61, 349–374.

Horst, T.W., Weil, J.C., 1992. Footprint estimation for scalar flux measurements in the atmospheric surface-layer. Bound.-Layer Meteorol. 59, 279–296.

Kljun, N., Rotach, M.W., Schmid, H.P., 2002. A three-dimensional backward Lagrangian footprint model for a wide range of boundary-layer stratifications. Bound.-Layer Meteorol. 103, 205–226.

Leclerc, M.Y., Thurtell, G.W., 1990. Footprint prediction of scalar fluxes using a Markovian analysis. Bound.-Layer Meteorol. 52, 247–258.

Lee, X., 2003. Fetch and footprint of turbulent fluxes over vegetative stands with elevated sources. Bound.-Layer Meteorol. 107, 561–579.

Legg, B.J., Raupach, M.R., Coppin, P.A., 1986. Experiments on scalar dispersion within a model plant canopy. Part III. An elevated line source. Bound.-Layer Meteorol. 35, 277–302.

Leuning, R., 2000. Estimation of scalar source/sink distributions in plant canopies using Lagrangian dispersion analysis: corrections for atmospheric stability and comparison with a multilayer canopy model. Bound.-Layer Meteorol. 96, 293–314.

Patankar, S.V., 1980. Numerical Heat Transfer and Fluid Flow. Taylor and Francis, 197 pp.

Rannik, Ü., Aubinet, M., Kurbanmuradov, O., Sabelfeld, K.K., Markkanen, T., Vesala, T., 2002. Footprint analysis for measurements over a heterogeneous forest. Bound.-Layer Meteorol. 97, 137–166.

Raupach, M.R., 1989. A practical Lagrangian method for relating scalar concentrations to source distributions in vegetation canopies. Quart. J. R. Meteorol. Soc. 115, 609–632.

Raupach, M.R., Coppin, P.A., Legg, B.J., 1986. Experiments on scalar dispersion within a model plant canopy. Part I. The turbulence structure. Bound.-Layer Meteorol. 35, 21–52.

Schmid, H.P., 1994. Source areas for scalar and scalar fluxes. Bound.-Layer Meteorol. 67, 293–318.

Strong, C., Fuentes, J.D., Baldocchi, D., 2004. Reactive hydrocarbon flux footprints during canopy senescence. Agric. For. Meteorol. 127, 159–173.

Warland, J., Thurtell, G.E., 2000. A Lagrangian solution to the relationship between a distributed source and concentration profile. Bound.-Layer Meteorol. 96, 453–471.